NANO LETTERS

ACS AUTHORCHOICE

pubs.acs.org/NanoLett

Letter

Unusual Spectral Diffusion of Single $CuInS_2$ Quantum Dots Sheds Light on the Mechanism of Radiative Decay

Stijn O. M. Hinterding, Mark J. J. Mangnus, P. Tim Prins, Huygen J. Jöbsis, Serena Busatto, Daniël Vanmaekelbergh, Celso de Mello Donega, and Freddy T. Rabouw*

Cite This: *Nano Lett.* 2021, 21, 658–665

Read Online

ACCESS | Metrics & More | Article Recommendations | Supporting Information

ABSTRACT: The luminescence of $CuInS_2$ quantum dots (QDs) is slower and spectrally broader than that of many other types of QDs. The origin of this anomalous behavior is still under debate. Single-QD experiments could help settle this debate, but studies by different groups have yielded conflicting results. Here, we study the photophysics of single core-only $CuInS_2$ and core/shell $CuInS_2$/CdS QDs. Both types of single QDs exhibit broad PL spectra with fluctuating peak position and single-exponential photoluminescence decay with a slow but fluctuating lifetime. Spectral diffusion of $CuInS_2$-based QDs is qualitatively and quantitatively different from CdSe-based QDs. The differences reflect the dipole moment of the $CuInS_2$ excited state and hole localization on a preferred site in the QD. Our results unravel the highly dynamic photophysics of $CuInS_2$ QDs and highlight the power of the analysis of single-QD property fluctuations.

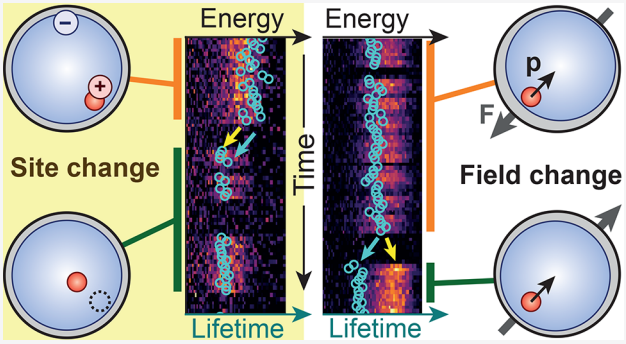

KEYWORDS: *Quantum dots, single-quantum-dot spectroscopy, $CuInS_2$, spectral diffusion*

Semiconductor nanocrystals (quantum dots, QDs) are promising luminophores for use in numerous applications, such as displays and bioimaging.[1] While CdSe- and perovskite-based QDs are most studied, Cd- and Pb-free alternatives have also seen rapid development in recent years. QDs based on $CuInS_2$ (CIS) are one of these alternatives.[2,3] They are particularly interesting for use in luminescent solar concentrators[4−10] as they exhibit large global Stokes shifts, minimizing reabsorption losses. This peculiar property, along with broad photoluminescence (PL) line widths (ensemble full-width at half-maximum, fwhm ∼400 meV)[11] and slow multiexponential PL decay (PL lifetime ∼200−400 ns),[11] shows that the photophysics of CIS QDs differs qualitatively from those of other types of QDs. In most other types of QDs (e.g., those based on CdSe, lead chalcogenide, or perovskite), luminescence occurs through recombination of delocalized quantum-confined electrons and holes.[12] In contrast, no consensus has yet been reached on the luminescence mechanism of CIS QDs and a number of different mechanisms have been proposed.[13−26,] Recent optical transient absorption,[17,19,20,22,27] X-ray transient absorption,[28] and electrochemical[29−31] studies strongly support a mechanism in which a delocalized electron recombines with a localized hole although other mechanisms are still claimed.[32,33] Striking similarities between the PL properties of CIS, Cu^+:CdSe, and Cu^+:InP suggest that the hole localizes on a Cu atom.[34]

Single-particle spectroscopy has been proven essential to understand various aspects of the photophysics of QDs, as it yields data that are not obscured by ensemble-averaging.[35−38] Unfortunately, CIS QDs are notoriously unstable under the harsh excitation conditions used in single-QD experiments.[23,26] Consequently, single-particle studies on CIS-based QDs are scarce[23,26,39,40] and achieve limited data quality compared to studies on other types of QDs. Most strikingly, Whitham et al. reported broad single-QD PL line widths (minimum fwhm, 190 meV) from individual core/shell CIS/CdS QDs,[23] whereas Zang et al. found narrow PL line widths (minimum fwhm, 60 meV) from individual core/shell CIS/ZnS QDs.[26] A possible origin for these contrasting results is interdiffusion of Cu^+ and Zn^{2+} during overgrowth of a ZnS shell on CIS QDs,[41] as these two elements (in contrast to Cd^{2+}) have similar ionic radii.[42] The limited and conflicting data make it difficult to draw definite conclusions on the intrinsic photophysics of CIS nanomaterials.

Here, we study the PL properties of individual core-only CIS and core/shell CIS/CdS QDs. Careful sample optimization

Received: October 23, 2020
Revised: December 28, 2020
Published: January 4, 2021

https://dx.doi.org/10.1021/acs.nanolett.0c04239
Nano Lett. 2021, 21, 658−665

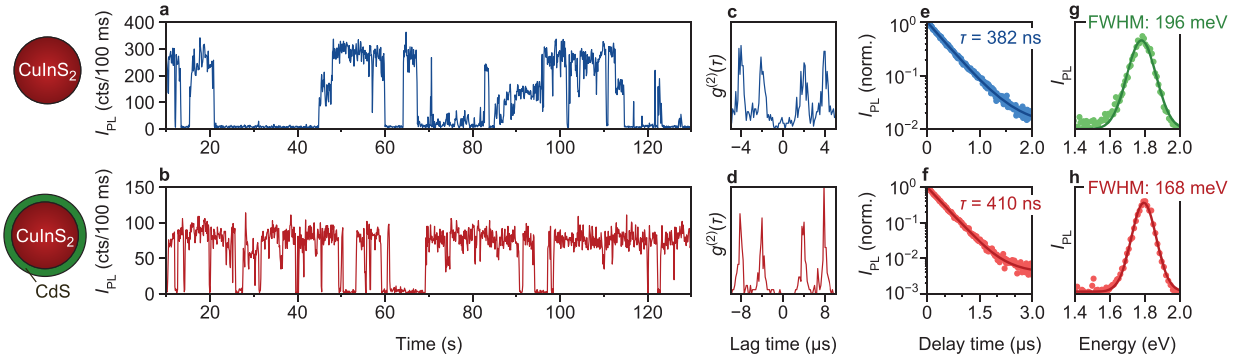

Figure 1. Top row, results from single-QD measurements on two different core-only CIS QDs; bottom row, results from similar experiments on one CIS/CdS core/shell QD. (a,b) PL intensity I_{PL} as a function of time. (c,d) Second-order correlation function $g^{(2)}(\tau)$. (e,f) PL decay curve, constructed from time periods in which the QD was ON [(e) $I_{PL} \geq 200$ cts/100 ms, (f) $I_{PL} \geq 65$ cts/100 ms]. Lines are fits to single-exponential decay with a constant background. (g,h) ON-state PL spectrum, integrated over (g) 6.5 s and (h) 91.3 s. Lines are Gaussian fits. As indicated by the color, data in panel g were measured on a different core-only CIS QD than the data depicted in panels a, c, and e.

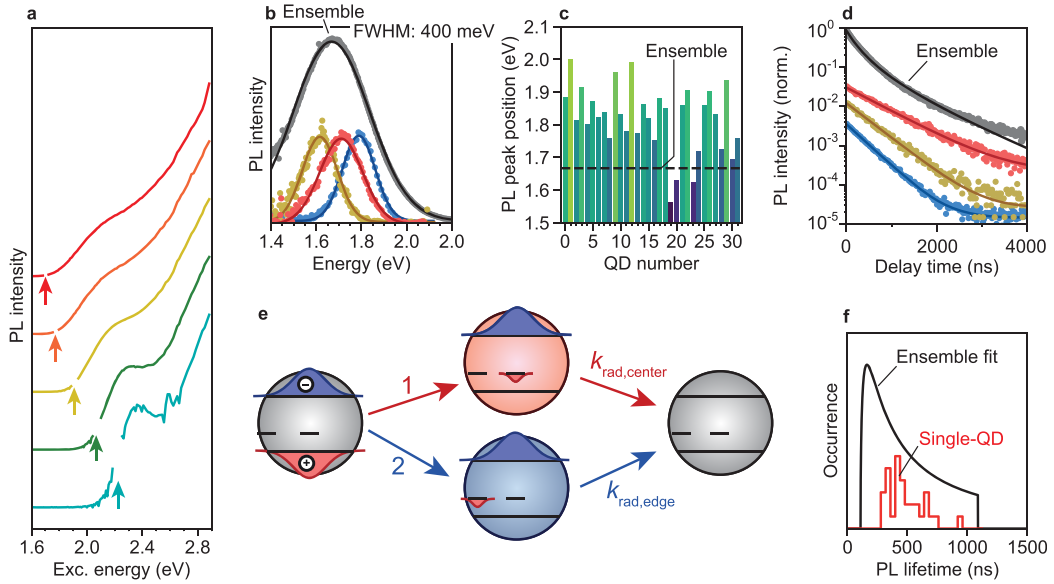

Figure 2. (a) Excitation spectra of an ensemble of CIS/CdS QDs dispersed in toluene. Each excitation spectrum was recorded for a different detection energy, as indicated by the arrows: (bottom, cyan) 2.226 eV, (green) 2.066 eV, (yellow) 1.907 eV, (orange) 1.771 eV, (top, red) 1.698 eV. (b) PL spectra of (black) an ensemble of CIS/CdS QDs dispersed in toluene, and (red, yellow, blue) single CIS/CdS QDs immobilized on a glass coverslip. Lines are fits to Gaussian peaks. (c) Fitted PL peak positions of all 32 core/shell CIS/CdS QDs that were studied. The dotted line indicates the fitted ensemble PL peak position. (d) PL decay curve of (top, black) an ensemble of CIS/CdS QDs dispersed in toluene and (red, yellow, blue) single CIS/CdS QDs. Red, yellow, and blue lines are single-exponential fits, whereas the black line is a fit to the model incorporating variations in the hole localization site (see SI, Section S2). (e) Schematic depiction of hole localization at a random Cu site (which, potentially, may be any Cu^+ ion present in the nanocrystal) after each excitation. The radiative decay rate of the excited state is determined by the electron−hole wave function overlap and thus by the location of the hole. (f) Distribution of PL lifetimes, obtained by (black) fitting the PL decay curve of an ensemble of CIS/CdS QDs [black curve in panel d] with a model incorporating an ensemble-wide distribution of hole localization sites, leading to a distribution of radiative decay rates (see SI, Section S2 for details) and (red) histogramming the ON-state average lifetimes of the 32 single QDs studied.

allows us to measure single-QD PL of both core-only CIS and core/shell CIS/CdS QDs for several minutes before irreversible photobleaching. We establish that the intrinsic PL properties of core-only CIS QDs are retained in core/shell CIS/CdS QDs. Variations between individual core/shell CIS/CdS QDs show the effect of inhomogeneous broadening on PL ensemble spectra and decay dynamics. Fluctuations in single-QD PL properties over time scales of seconds to minutes provide insight into the emission mechanism. Spectral diffusion in CIS QDs is quantitatively and qualitatively different from that reported for CdSe QDs, consistent with radiative recombination of a delocalized electron with a Cu-localized hole. The correlations between the fluctuating PL peak position and PL lifetime provide evidence that the hole always localizes on a preferential Cu site in the QD. For a few QDs, we observe that the preferential Cu site changes. Quantum-mechanical calculations show that the dipolar character of the excited state underlies the strong fluctuations in PL energy and lifetime. These new insights into the emission mechanism of CIS-based QDs will be useful for the optimization of the optoelectronic properties of this class of materials.

We study core-only chalcopyrite CIS QDs of ∼2.4 nm. These QDs are Cu-rich (atomic ratio Cu/In = 1.0:0.78). The

https://dx.doi.org/10.1021/acs.nanolett.0c04239
Nano Lett. 2021, 21, 658−665

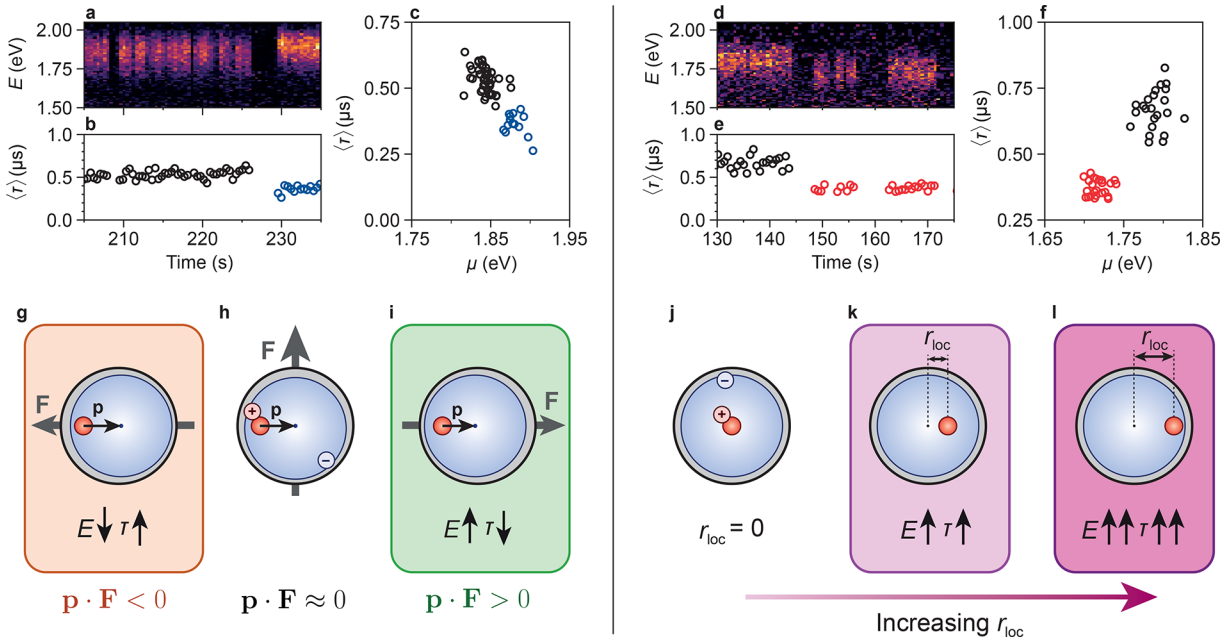

Figure 3. Single-QD (a) PL spectra and (b) average photon delay time $\langle\tau\rangle$, as a function of time. (c) Correlation of average photon delay time $\langle\tau\rangle$ and fitted peak position μ. The color scale in panel a (black to purple to yellow) indicates PL intensity. (d–f) The same as in panels a–c but for a different QD. (g–i) Schematic depiction of spectral diffusion induced by the quantum-confined Stark effect. Mobile surface atoms or ligands create a fluctuating electric field **F**. We depict three possible orientations with respect to the excited-state dipole **p**: (g) antiparallel, (h) orthogonal, and (i) parallel. (j–l) Schematic depiction of spectral diffusion due to changes in the hole localization site r_{loc}. Effects on the exciton energy E and lifetime τ are indicated in the cartoons.

core/shell CIS/CdS QDs exhibit the same crystal structure with an estimated particle size of 3.0 nm. Both samples are polydisperse (see Supporting Information (SI), Section S2 for details). An earlier study found that these QDs exhibit a tetrahedral shape.[22] Our sample preparation procedure (SI, Section S1) allowed for single-QD measurements for several minutes before photobleaching.

Figure 1 compares the single-QD PL properties of core-only CIS and core/shell CIS/CdS QDs. Both core-only CIS and core/shell CIS/CdS QDs exhibit PL blinking, characterized by fluctuations between periods of high intensity and periods of lower intensity (Figure 1a,b). Many QDs exhibit PL blinking with intermediate intensities that are difficult to categorize (e.g., SI, Extended Data Figures E10 and E22). In some QDs, the lower-intensity periods are due to quenching by trapping of charge carriers from the band edge (e.g., SI, Extended Data Figures E7 and E43).[43] These charge carriers are likely electrons, as the hole localizes on subpicosecond time scales.[22] In other QDs, quenching occurs through trapping of hot charge carriers ("B-type blinking"; for example, SI, Extended Data Figures E16 and E27).[36] Both core-only CIS and core/shell CIS/CdS QDs are single-photon emitters, as evidenced by antibunching in the second-order correlation function $g^{(2)}(\tau)$ (Figure 1c,d). In the absence of spectral diffusion, the PL decay of the ON-state of these QDs is single-exponential (Figure 1e,f). We observe broad PL line widths for both the core-only CIS and core/shell CIS/CdS QDs (Figure 1g,h; lowest fwhm of all studied QDs: 179 and 157 meV, respectively; see Tables S1 and S2). From the similarity between the optical properties of these two types of QDs, we conclude that the intrinsic PL properties of core-only CIS are retained in core/shell CIS/CdS QDs. This is expected because the CIS core material should be unaffected by CdS shelling, as a large mismatch in ionic radii prevents Cu^+ and Cd^{2+} interdiffusion.[42]

Ensemble-scale measurements on CIS and CIS/CdS QDs are strongly influenced by sample inhomogeneity. For example, absorption and excitation spectra of CIS and CIS/CdS QD dispersions are generally featureless (Figure S2).[6,8,21−24,26,29,31,32,41,44,9,45,46,10,14,16−20] However, excitation spectra of CIS/CdS QD subensembles, resolved by detecting PL at distinct, narrow energy ranges, exhibit clear band-edge transition features (Figure 2a). Sample inhomogeneities become even more apparent when comparing single-QD properties to those of the ensemble. The single-QD PL line widths of core-only CIS (Table S1; SI, Extended Data Figures E1−E6) and core/shell CIS/CdS QDs (Figure 2b; Table S2; SI, Extended Data Figures E17−E48) are approximately two times narrower than the ensemble line width. Indeed, the PL peak positions of the individual QDs studied are widely distributed (Figure 2c). The origin of sample inhomogeneity may be manifold, including polydispersity in size, shape, and composition.[14,24,27,47] In addition, as we will show and discuss in more detail below, inhomogeneous broadening is enhanced as a result of the peculiar emission mechanism of CIS QDs involving a Cu-localized hole and a dipolar excited state.

Variations in the PL lifetime between single QDs (Figure 2d) provide insight into the emission mechanism. Transient absorption[17,19,20,22,27] and spectroelectrochemical[29−31] studies have established that luminescence in CIS-based nanomaterials involves the radiative recombination of a delocalized electron with a localized hole. One can envision two different mechanisms of PL decay via Cu centers, which would be indistinguishable in ensemble-scale measurements but yield different results at the single-QD level. In the first mechanism, after each excitation the hole may localize at any of the Cu^+ ions present in the QD (Figure 2e).[48] Such behavior would

https://dx.doi.org/10.1021/acs.nanolett.0c04239
Nano Lett. 2021, 21, 658−665

lead to multiexponential decay dynamics on the single-QD scale, as the localization site of the hole affects the electron−hole wave function overlap and thus the radiative lifetime.[11,12] Alternatively, the hole may always localize at one specific Cu site in the QD, perhaps because of the presence of a nearby defect[26] or electrostatic interactions with the QD surface.[25] This scenario would lead to single-exponential decay of single-QD PL, as the electron−hole overlap and thereby radiative decay rate is the same after each excitation. The near-single-exponential character of single-QD PL decay curves indicates that one specific Cu site (or at most a few) is active in a QD at any given time, and that the hole does not move between Cu sites on the time scale of emission. The distribution of single-QD lifetimes is consistent with a distribution of the localization site over the QD ensemble, resulting in an ensemble-wide distribution of radiative lifetimes (Figure 2f; SI, Section S2).[26] However, it is important to realize that the single-QD PL decay curve would be virtually indistinguishable from single-exponential decay, especially in the case of noisy data, if a few hole localization sites were active with not so dissimilar lifetimes. Although our data does not allow us to conclude what distinguishes a "favorite" localization site from any other Cu site, we speculate that a nearby defect or surface charge could provide some charge stabilization, thereby attracting the hole. Indeed, DFT calculations have shown that the presence of surface charges can determine where the hole localizes.[25] A preferential site could also be distinguished by a slight change in the local atomic arrangement: if the local structure is distorted in such a way that it more closely resembles the arrangement after hole localization, this could decrease a possible activation barrier involved in hole localization, thereby favoring localization at this specific site.

Fluctuations of the PL spectrum and lifetime of single QDs, and correlations therein, reveal surprising dynamics of hole localization and their significant effect on the broadening of the ensemble properties. Our single core/shell CIS/CdS QDs are sufficiently photostable to allow for the simultaneous measurement of their PL decay curve and PL spectrum at a 100 ms temporal resolution. SI Extended Data Figures E17−E48 provide a complete overview of the measurements on 32 core/shell CIS/CdS QDs.

First, some QDs show no spectral diffusion at all (e.g., Extended Data, Figures E21 and E44). Still, such QDs exhibit broad PL spectra with fwhm on the order of 160−170 meV (Table S2). In comparison, single CdSe-based QDs generally exhibit fwhm of 50−60 meV.[49,50] Clearly, broad PL line widths in CIS-based QDs are not due to time averaging and spectral diffusion. Instead, they are intrinsic to these nanomaterials and likely due to strong electron−phonon coupling.[51] Such broad single-particle PL spectra cannot be explained by a mechanism involving the recombination of a delocalized exciton.[15,33]

Figure 3 summarizes two different types of fluctuations that we observed in other QDs: (i) spectral diffusion wherein higher PL peak energies are correlated with shorter PL lifetimes (Figure 3a−c), and (ii) spectral diffusion wherein higher PL peak energies are correlated with longer PL lifetimes (Figure 3d−f). Additionally, some QDs exhibit spectral diffusion without a clear correlation between PL lifetime and PL peak energy (see, e.g., Extended Data, Figures E33, E40, and E48), possibly because both types of fluctuations occur simultaneously.

Type-1 spectral diffusion with a "negative" correlation between peak energy and PL lifetime (Figure 3a−c; higher energies correlate with shorter lifetimes) is known from experiments on CdSe-based nanocrystals. However, the fluctuations in our CIS/CdS QDs are significantly stronger. The PL peak positions of our CIS/CdS QDs fluctuate on average over a range of 110 meV with some QDs exhibiting fluctuations in excess of 200 meV (see Table S2), whereas CdSe-based nanocrystals show spectral diffusion over at most a few tens of millielectronvolts.[49,50,52] Even more striking, type-2 spectral diffusion with a "positive" correlation between peak energy and PL lifetime (Figure 3d−f; higher energies correlate with longer lifetimes) is never observed for CdSe-based nanocrystals.[49,50]

We will show below that both anomalies of the spectral diffusion of CIS/CdS QDs are a direct signature of the peculiar emission mechanism. The excited-state energy of a QD can be written as

$$E = E_g + V_C + \mathbf{p}\cdot\mathbf{F} - \frac{1}{2}\alpha F^2 \quad (1)$$

where E_g is the single-particle gap (i.e., sum of electron and hole energies), V_C is the Coulomb interaction between charge carriers including dielectric effects, $\mathbf{p}$ is the static dipole moment of the excited state, and α is the exciton polarizability (see SI, Section S3 for a derivation). $\mathbf{F}$ is the electric field that the excited state experiences due to charges at the surface of the QD, which can be due to missing ligands or dangling bonds. "Conventional" spectral diffusion of CdSe-based nanocrystals is explained in terms of the quantum-confined Stark effect (QCSE),[49,50,52,53] induced by spontaneous fluctuations in $\mathbf{F}$ due to the mobility of the surface charges. Experiments with applied external fields on type-I CdSe-based nanocrystals have revealed a dominant contribution of the quadratic term in the resulting change of the exciton energy E: Stark shifts due to the exciton polarizability α.[53,54] This effect induces a negative correlation between PL peak energy and PL lifetime, as polarization of the exciton increases the radiative lifetime.[49,50] CIS-based QDs are different from CdSe in three ways because of hole localization: (1) V_C depends strongly on the location r_{loc} of the hole, (2) $\mathbf{p}$ can be large if the hole localizes off-center, (3) α is significantly smaller as the localized hole is not polarizable (SI, Section S3). Some QDs exhibit a (slight) anticorrelation between fitted fwhm and peak position (e.g., Extended Data, Figure E49a,p,w). This indicates that external fields may also influence electron−phonon coupling and thereby the Stokes shift. However, as this effect appears to be minimal, we ignore its contribution to fluctuations in the emission energy in our further discussion.

We developed a simple effective-mass model, where we approximate the CIS QD as a spherical infinite potential well with radius a. In our model, the hole resides on specific localization sites, while the electron is delocalized over the entire particle. We consider the possibility of spectral diffusion due to a fluctuating external electric field $\mathbf{F}$ that interacts with the exciton wave function (i.e., the QCSE), as well as a changing hole localization site.

On the basis of our calculations, we can understand how the qualitatively and quantitatively different spectral diffusion behavior of CIS-based QDs is a consequence of hole localization. We can attribute type-1 spectral diffusion, that is, a negative correlation between peak energy and PL lifetime, to the QCSE due to fluctuating $\mathbf{F}$ (see schematic depiction in Figure 3g−i). The response of the peak energy to $\mathbf{F}$ can be much stronger than in CdSe-based QDs, because the CIS

https://dx.doi.org/10.1021/acs.nanolett.0c04239
Nano Lett. 2021, 21, 658−665

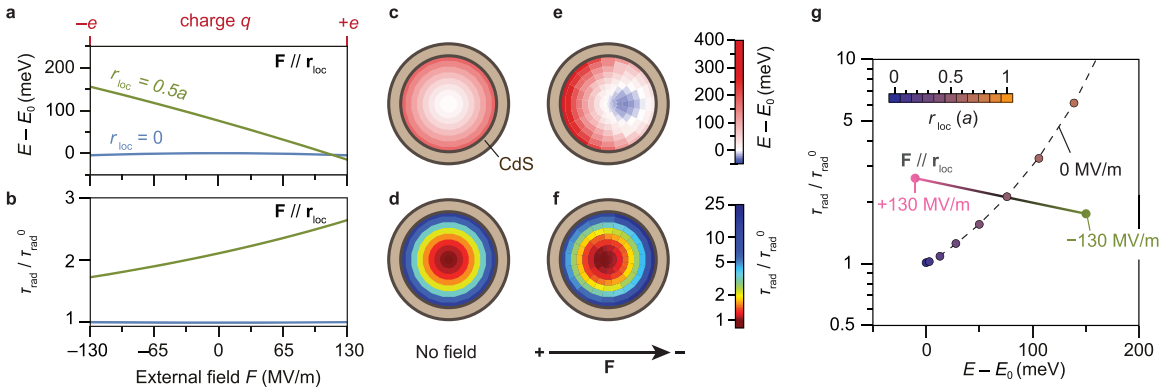

Figure 4. Results from quantum-mechanical calculations showing (a) the change in exciton energy $E-E_0$ and (b) normalized radiative lifetime τ_{rad}/τ_{rad}^0, as a function of external electric field. Here, E_0 and τ_{rad}^0 are the excited-state energy and radiative lifetime for $r_{loc} = 0$ and $\mathbf{F} = 0$. Lines correspond to hole localization (blue) at the center of the QD and (green) at $r_{loc} = 0.5a$, where a is the QD radius. We consider fields $\mathbf{F}$ oriented along $\mathbf{r}_{loc}$. (c−f) Results from the same model, depicting in color scale how the location of hole localization affects (c,e) the exciton energy and (d,f) the radiative lifetime with (c,d) no external field and (e,f) an external field of +130 MV/m in the horizontal direction. (g) The same results as in panels (a−d) but now showing correlations between lifetime and energy. The solid pink−green line shows the relation between τ_{rad}/τ_{rad}^0 and $E-E_0$ for hole localization at $0.5a$ with a varying external field from (pink) +130 MV/m to (green) −130 MV/m. The dashed line considers hole localization at increasing r_{loc}, indicated by the colored circles, without external field. The more complex relationship of τ_{rad}/τ_{rad}^0 and $E-E_0$ for varying r_{loc} with an external field of 130 MV/m is depicted in Figure S5. Spectral diffusion in excess of 200 meV, observed in some QDs, is likely due to fluctuating electric fields stronger than 130 MV/m, which may occur occasionally in smaller particles.

exciton can have a large dipole moment $\mathbf{p} = e\cdot\mathbf{r}_{loc}$ (where e is the elementary charge). Indeed, our effective-mass model confirms that the dependence of E on $\mathbf{F}$ depends strongly on $\mathbf{r}_{loc}$ (Figure 4a). The same holds for the radiative decay rate (see Figure 4b). The dipolar nature of the excited state, arising from the hole localizing at a preferential Cu^+ ion inside the QD, is thus responsible for the strong spectral diffusion in CIS/CdS QDs. The observation of type-1 spectral diffusion on time scales of seconds implies that $\mathbf{F}$ fluctuates on these time scales (as is common in CdSe-based QDs) while $\mathbf{r}_{loc}$ is fixed. That means, the hole must localize on the same Cu site over millions of consecutive photocycles. If it did not, the linear term in eq 1 would average out to $\langle\mathbf{p}\cdot\mathbf{F}\rangle = 0$ independent of $\mathbf{F}$. This agrees well with the single-exponential PL decay in absence of spectral diffusion (see Figure 2 and corresponding discussion).

While fluctuations in $\mathbf{F}$ explain type-1 spectral diffusion (see Figure 3g−i), they cannot explain type-2 spectral diffusion (i.e., with positive correlations between energy and lifetime). Instead, type-2 spectral diffusion requires fluctuations in r_{loc} on the time scale of seconds (depicted schematically in Figure 3j−l). The dominant contribution to the energy change comes from V_C. As the hole localization site moves toward the edge of the QD, V_C becomes less negative, increasing the excited-state energy (Figure 4c; Supporting Information, Section S3). Likewise, the electron−hole wave function overlap is decreased, increasing the radiative lifetime (Figure 4d). The situation is somewhat more complex if r_{loc} changes in the presence of an external field (Figure 4e,f). In most cases, this produces a positive correlation of changes in energy and lifetime (Figure 4g) but for some scenarios a negative correlation can occur (Figure S5). However, clearly, the alternative model of a QCSE due to fluctuating $\mathbf{F}$ (pink-green curve in Figure 4g) cannot produce positive correlations. We thus attribute type-2 spectral diffusion events with a positive correlation between emission energy and PL lifetime to a spontaneous change in r_{loc}, that is, the Cu site at which the hole preferentially localizes.

A change in $\mathbf{r}_{loc}$ need not involve a change in the inorganic crystalline part of the QD; DFT calculations have shown that the position at which the hole localizes can be strongly influenced by the presence of charges on the QD surface.[25] This may explain why some QDs exhibit spectral diffusion without a correlation between PL lifetime and PL peak position: (movement of) surface charges may induce both the QCSE and simultaneously a change in the hole localization site, resulting in an unclear net correlation. We observe clear type-2 spectral diffusion in only 3 of the 32 CIS/CdS QDs studied. Together, fluctuations of $\mathbf{F}$ and $\mathbf{r}_{loc}$, possibly correlated, can produce complex and strong fluctuations of exciton energy and PL lifetime, as we observe experimentally.

In summary, our single-QD experiments have shown how sample inhomogeneities determine the broad PL line widths and multiexponential PL decay of CIS nanomaterials. Even in the absence of spectral diffusion, the PL line width of CIS/CdS QDs is broad (minimum fwhm >0.16 eV). This points to electron−phonon coupling, which is, along with the long PL lifetimes, consistent with hole localization prior to radiative recombination. Additionally, the PL decay is single-exponential in the absence of spectral diffusion, suggesting that the hole localizes at the same Cu site after each excitation. Most QDs exhibit spectral diffusion to a much stronger extent (with shifts in excess of 200 meV) than previously observed in CdSe-based nanomaterials. We observe two types of spectral diffusion. First, spectral diffusion due to the QCSE is much stronger than in CdSe because the CIS electron−hole pair has a dipole moment. Second, changes in the hole localization site account for a spectral diffusion mechanism unique to CIS. A combination of factors, involving QD size, shape, composition, and surface-ligand coverage likely determines at which Cu site the hole preferentially localizes. In all, our results highlight how emission fluctuations provide valuable information on the photophysics of QDs. Similar experiments on InP QDs may shed light on the recent claim that trapped charge carriers are involved in the fluorescence mechanism.[55]

https://dx.doi.org/10.1021/acs.nanolett.0c04239
Nano Lett. 2021, 21, 658−665

■ ASSOCIATED CONTENT

Supporting Information

The Supporting Information is available free of charge at https://pubs.acs.org/doi/10.1021/acs.nanolett.0c04239.

Experimental methods, further details related to the data processing, analysis and modeling, derivations and details on the quantum-mechanical calculations, ensemble-scale characterization of the two samples, tables summarizing the observed properties of all studied QDs; Extended Data shows overview of single-CIS-QD and single-CIS/CdS-QD results for all QDs studied; software program used in our time-correlated single-photon counting measurements for data acquisition, visualization, and storage is available online[56] free of charge.(PDF)

■ AUTHOR INFORMATION

Corresponding Author

Freddy T. Rabouw − *Soft Condensed Matter, Debye Institute for Nanomaterials Science and Inorganic Chemistry and Catalysis, Debye Institute for Nanomaterials Science, Utrecht University, 3584CC Utrecht, The Netherlands;* orcid.org/0000-0002-4775-0859; Email: f.t.rabouw@uu.nl

Authors

Stijn O. M. Hinterding − *Soft Condensed Matter, Debye Institute for Nanomaterials Science and Inorganic Chemistry and Catalysis, Debye Institute for Nanomaterials Science, Utrecht University, 3584CC Utrecht, The Netherlands;* orcid.org/0000-0002-3940-1253

Mark J. J. Mangnus − *Soft Condensed Matter, Debye Institute for Nanomaterials Science and Inorganic Chemistry and Catalysis, Debye Institute for Nanomaterials Science, Utrecht University, 3584CC Utrecht, The Netherlands;* orcid.org/0000-0002-3595-8097

P. Tim Prins − *Condensed Matter and Interfaces, Debye Institute for Nanomaterials Science, Utrecht University, 3584CC Utrecht, The Netherlands;* orcid.org/0000-0002-8258-0074

Huygen J. Jöbsis − *Condensed Matter and Interfaces, Debye Institute for Nanomaterials Science, Utrecht University, 3584CC Utrecht, The Netherlands*

Serena Busatto − *Condensed Matter and Interfaces, Debye Institute for Nanomaterials Science, Utrecht University, 3584CC Utrecht, The Netherlands*

Daniël Vanmaekelbergh − *Condensed Matter and Interfaces, Debye Institute for Nanomaterials Science, Utrecht University, 3584CC Utrecht, The Netherlands;* orcid.org/0000-0002-3535-8366

Celso de Mello Donega − *Condensed Matter and Interfaces, Debye Institute for Nanomaterials Science, Utrecht University, 3584CC Utrecht, The Netherlands;* orcid.org/0000-0002-4403-3627

Complete contact information is available at: https://pubs.acs.org/10.1021/acs.nanolett.0c04239

Author Contributions

The manuscript was written through contributions of all authors. All authors have given approval to the final version of the manuscript.

Notes

The authors declare no competing financial interest.

■ ACKNOWLEDGMENTS

This work was supported by The Netherlands Center for Multiscale Catalytic Energy Conversion (MCEC), an NWO Gravitation Programme funded by the Ministry of Education, Culture, and Science of the government of The Netherlands. P.T.P., H.J.J., D.V., and C.M.D. acknowledge support from The Netherlands Organization for Scientific Research (NWO, Grant 14614 "Q-Lumicon"). F.T.R. acknowledges financial support from The Netherlands Organization for Scientific Research NWO (VENI Grant 722.017.002). The authors thank the SOLEIL synchrotron, Saint-Aubin, France, for granting beamtime under proposal number 20181211. Javier Pérez is thanked for support during the synchrotron experiments.

■ REFERENCES

(1) Talapin, D. V.; Lee, J.; Kovalenko, M. V.; Shevchenko, E. V. Prospects of Colloidal Nanocrystals for Electronic and Optoelectronic Applications. *Chem. Rev.* **2010**, *110*, 389−458.

(2) Reiss, P.; Carrière, M.; Lincheneau, C.; Vaure, L.; Tamang, S. Synthesis of Semiconductor Nanocrystals, Focusing on Nontoxic and Earth-Abundant Materials. *Chem. Rev.* **2016**, *116*, 10731−10819.

(3) Van der Stam, W.; Berends, A. C.; De Mello Donegá, C. Prospects of Colloidal Copper Chalcogenide Nanocrystals. *ChemPhysChem* **2016**, *17*, 559−581.

(4) Meinardi, F.; McDaniel, H.; Carulli, F.; Colombo, A.; Velizhanin, K. A.; Makarov, N. S.; Simonutti, R.; Klimov, V. I.; Brovelli, S. Highly Efficient Large-Area Colourless Luminescent Solar Concentrators Using Heavy-Metal-Free Colloidal Quantum Dots. *Nat. Nanotechnol.* **2015**, *10*, 878−885.

(5) Knowles, K. E.; Kilburn, T. B.; Alzate, D. G.; McDowall, S.; Gamelin, D. R. Bright $CuInS_2$/CdS Nanocrystal Phosphors for High-Gain Full-Spectrum Luminescent Solar Concentrators. *Chem. Commun.* **2015**, *51*, 9129−9132.

(6) Bergren, M. R.; Makarov, N. S.; Ramasamy, K.; Jackson, A.; Guglielmetti, R.; McDaniel, H. High-Performance $CuInS_2$ Quantum Dot Laminated Glass Luminescent Solar Concentrators for Windows. *ACS Energy Lett.* **2018**, *3*, 520−525.

(7) Wu, K.; Li, H.; Klimov, V. I. Tandem Luminescent Solar Concentrators Based on Engineered Quantum Dots. *Nat. Photonics* **2018**, *12*, 105−110.

(8) Hu, X.; Kang, R.; Zhang, Y.; Deng, L.; Zhong, H.; Zou, B.; Shi, L.-J. Ray-Trace Simulation of $CuInS(Se)_2$ Quantum Dot Based Luminescent Solar Concentrators. *Opt. Express* **2015**, *23*, A858−A867.

(9) Li, C.; Chen, W.; Wu, D.; Quan, D.; Zhou, Z.; Hao, J.; Qin, J.; Li, Y.; He, Z.; Wang, K. Large Stokes Shift and High Efficiency Luminescent Solar Concentrator Incorporated with $CuInS_2$/ZnS Quantum Dots. *Sci. Rep.* **2016**, *5*, 17777.

(10) Sumner, R.; Eiselt, S.; Kilburn, T. B.; Erickson, C.; Carlson, B.; Gamelin, D. R.; McDowall, S.; Patrick, D. L. Analysis of Optical Losses in High-Efficiency $CuInS_2$-Based Nanocrystal Luminescent Solar Concentrators: Balancing Absorption versus Scattering. *J. Phys. Chem. C* **2017**, *121*, 3252−3260.

(11) Berends, A. C.; Mangnus, M. J. J.; Xia, C.; Rabouw, F. T.; De Mello Donega, C. Optoelectronic Properties of Ternary I-III-VI_2 Semiconductor Nanocrystals: Bright Prospects with Elusive Origins. *J. Phys. Chem. Lett.* **2019**, *10*, 1600−1616.

(12) Rabouw, F. T.; De Mello Donega, C. Excited-State Dynamics in Colloidal Semiconductor Nanocrystals. *Top. Curr. Chem.* **2016**, *374*, 58.

(13) Seo, J.; Raut, S.; Abdel-Fattah, M.; Rice, Q.; Tabibi, B.; Rich, R.; Fudala, R.; Gryczynski, I.; Gryczynski, Z.; Kim, W.-J.; Jung, S.; Hyun, R. Time-Resolved and Temperature-Dependent Photoluminescence of Ternary and Quaternary Nanocrystals of $CuInS_2$ with ZnS Capping and Cation Exchange. *J. Appl. Phys.* **2013**, *114*, 094310.

(14) Chen, B.; Zhong, H.; Zhang, W.; Tan, Z.; Li, Y.; Yu, C.; Zhai, T.; Bando, Y.; Yang, S.; Zou, B. Highly Emissive and Color-Tunable $CuInS_2$-Based Colloidal Semiconductor Nanocrystals: Off-Stoichiometry Effects and Improved Electroluminescence Performance. *Adv. Funct. Mater.* **2012**, *22*, 2081−2088.
(15) Shabaev, A.; Mehl, M. J.; Efros, A. L. Energy Band Structure of $CuInS_2$ and Optical Spectra of $CuInS_2$ Nanocrystals. *Phys. Rev. B: Condens. Matter Mater. Phys.* **2015**, *92*, 035431.
(16) Omata, T.; Nose, K.; Kurimoto, K.; Kita, M. Electronic Transition Responsible for Size-Dependent Photoluminescence of Colloidal $CuInS_2$ Quantum Dots. *J. Mater. Chem. C* **2014**, *2*, 6867−6872.
(17) Kraatz, I. T.; Booth, M.; Whitaker, B. J.; Nix, M. G. D.; Critchley, K. Sub-Bandgap Emission and Intraband Defect-Related Excited-State Dynamics in Colloidal $CuInS_2$/ZnS Quantum Dots Revealed by Femtosecond Pump-Dump-Probe Spectroscopy. *J. Phys. Chem. C* **2014**, *118*, 24102−24109.
(18) Leach, A. D. P.; Macdonald, J. E. Optoelectronic Properties of $CuInS_2$ Nanocrystals and Their Origin. *J. Phys. Chem. Lett.* **2016**, *7*, 572−583.
(19) Li, L.; Pandey, A.; Werder, D. J.; Khanal, B. P.; Pietryga, J. M.; Klimov, V. I. Efficient Synthesis of Highly Luminescent Copper Indium Sulfide-Based Core/Shell Nanocrystals with Surprisingly Long-Lived Emission. *J. Am. Chem. Soc.* **2011**, *133*, 1176−1179.
(20) Sun, J.; Zhu, D.; Zhao, J.; Ikezawa, M.; Wang, X.; Masumoto, Y. Ultrafast Carrier Dynamics in $CuInS_2$ Quantum Dots. *Appl. Phys. Lett.* **2014**, *104*, 023118.
(21) Knowles, K. E.; Nelson, H. D.; Kilburn, T. B.; Gamelin, D. R. Singlet-Triplet Splittings in the Luminescent Excited States of Colloidal Cu^+:CdSe, Cu^+:InP, and $CuInS_2$ Nanocrystals: Charge-Transfer Configurations and Self-Trapped Excitons. *J. Am. Chem. Soc.* **2015**, *137*, 13138−13147.
(22) Berends, A. C.; Rabouw, F. T.; Spoor, F. C. M.; Bladt, E.; Grozema, F. C.; Houtepen, A. J.; Siebbeles, L. D. A.; De Mello Donegá, C. Radiative and Nonradiative Recombination in $CuInS_2$ Nanocrystals and $CuInS_2$-Based Core/Shell Nanocrystals. *J. Phys. Chem. Lett.* **2016**, *7*, 3503−3509.
(23) Whitham, P. J.; Marchioro, A.; Knowles, K. E.; Kilburn, T. B.; Reid, P. J.; Gamelin, D. R. Single-Particle Photoluminescence Spectra, Blinking, and Delayed Luminescence of Colloidal $CuInS_2$ Nanocrystals. *J. Phys. Chem. C* **2016**, *120*, 17136−17142.
(24) Nagamine, G.; Nunciaroni, H. B.; McDaniel, H.; Efros, A. L.; De Brito Cruz, C. H.; Padilha, L. A. Evidence of Band-Edge Hole Levels Inversion in Spherical $CuInS_2$ Quantum Dots. *Nano Lett.* **2018**, *18*, 6353−6359.
(25) Nelson, H. D.; Gamelin, D. R. Valence-Band Electronic Structures of Cu^+-Doped ZnS, Alloyed Cu-In-Zn-S, and Ternary $CuInS_2$ Nanocrystals: A Unified Description of Photoluminescence across Compositions. *J. Phys. Chem. C* **2018**, *122*, 18124−18133.
(26) Zang, H.; Li, H.; Makarov, N. S.; Velizhanin, K. A.; Wu, K.; Park, Y.-S.; Klimov, V. I. Thick-Shell $CuInS_2$/ZnS Quantum Dots with Suppressed "Blinking" and Narrow Single-Particle Emission Line Widths. *Nano Lett.* **2017**, *17*, 1787−1795.
(27) Fuhr, A.; Yun, H. J.; Crooker, S. A.; Klimov, V. I. Spectroscopic and Magneto-Optical Signatures of Cu^{1+} and Cu^{2+} Defects in Copper Indium Sulfide Quantum Dots. *ACS Nano* **2020**, *14*, 2212−2223.
(28) Hu, W.; Ludwig, J.; Pattengale, B.; Yang, S.; Liu, C.; Zuo, X.; Zhang, X.; Huang, J. Unravelling the Correlation of Electronic Structure and Carrier Dynamics in $CuInS_2$ Nanoparticles. *J. Phys. Chem. C* **2018**, *122*, 974−980.
(29) Fuhr, A. S.; Yun, H. J.; Makarov, N. S.; Li, H.; McDaniel, H.; Klimov, V. I. Light Emission Mechanisms in $CuInS_2$ Quantum Dots Evaluated by Spectral Electrochemistry. *ACS Photonics* **2017**, *4*, 2425−2435.
(30) Van der Stam, W.; De Graaf, M.; Gudjonsdottir, S.; Geuchies, J. J.; Dijkema, J. J.; Kirkwood, N.; Evers, W. H.; Longo, A.; Houtepen, A. J. Tuning and Probing the Distribution of Cu^+ and Cu^{2+} Trap States Responsible for Broad-Band Photoluminescence in $CuInS_2$ Nanocrystals. *ACS Nano* **2018**, *12*, 11244−11253.
(31) Pinchetti, V.; Lorenzon, M.; McDaniel, H.; Lorenzi, R.; Meinardi, F.; Klimov, V. I.; Brovelli, S. Spectro-Electrochemical Probing of Intrinsic and Extrinsic Processes in Exciton Recombination in I-III-VI_2 Nanocrystals. *Nano Lett.* **2017**, *17*, 4508−4517.
(32) Debnath, T.; Ghosh, H. N. Ternary Metal Chalcogenides: Into the Exciton and Biexciton Dynamics. *J. Phys. Chem. Lett.* **2019**, *10*, 6227−6238.
(33) Anand, A.; Zaffalon, M. L.; Gariano, G.; Camellini, A.; Gandini, M.; Brescia, R.; Capitani, C.; Bruni, F.; Pinchetti, V.; Zavelani-Rossi, M.; Meinardi, F.; Crooker, S. A.; Brovelli, S. Evidence for the Band-Edge Exciton of $CuInS_2$ Nanocrystals Enables Record Efficient Large-Area Luminescent Solar Concentrators. *Adv. Funct. Mater.* **2020**, *30*, 1906629.
(34) Knowles, K. E.; Hartstein, K. H.; Kilburn, T. B.; Marchioro, A.; Nelson, H. D.; Whitham, P. J.; Gamelin, D. R. Luminescent Colloidal Semiconductor Nanocrystals Containing Copper: Synthesis, Photophysics, and Applications. *Chem. Rev.* **2016**, *116*, 10820−10851.
(35) Schwartz, O.; Tenne, R.; Levitt, J. M.; Deutsch, Z.; Itzhakov, S.; Oron, D. Colloidal Quantum Dots as Saturable Fluorophores. *ACS Nano* **2012**, *6*, 8778−8782.
(36) Galland, C.; Ghosh, Y.; Steinbrück, A.; Sykora, M.; Hollingsworth, J. A.; Klimov, V. I.; Htoon, H. Two Types of Luminescence Blinking Revealed by Spectroelectrochemistry of Single Quantum Dots. *Nature* **2011**, *479*, 203−207.
(37) Becker, M. A.; Vaxenburg, R.; Nedelcu, G.; Sercel, P. C.; Shabaev, A.; Mehl, M. J.; Michopoulos, J. G.; Lambrakos, S. G.; Bernstein, N.; Lyons, J. L.; Stöferle, T.; Mahrt, R. F.; Kovalenko, M. V.; Norris, D. J.; Rainò, G.; Efros, A. L. Bright Triplet Excitons in Caesium Lead Halide Perovskites. *Nature* **2018**, *553*, 189−193.
(38) Tamarat, P.; Bodnarchuk, M. I.; Trebbia, J. B.; Erni, R.; Kovalenko, M. V.; Even, J.; Lounis, B. The Ground Exciton State of Formamidinium Lead Bromide Perovskite Nanocrystals Is a Singlet Dark State. *Nat. Mater.* **2019**, *18*, 717−724.
(39) Zhang, A.; Dong, C.; Li, L.; Yin, J.; Liu, H.; Huang, X.; Ren, J. Non-Blinking (Zn)CuInS/ZnS Quantum Dots Prepared by In Situ Interfacial Alloying Approach. *Sci. Rep.* **2015**, *5*, 15227.
(40) Nguyen, A. T.; Gao, F.; Baucom, D.; Heyes, C. D. $CuInS_2$-Doped ZnS Quantum Dots Obtained via Non-Injection Cation Exchange Show Reduced but Heterogeneous Blinking and Provide Insights into Their Structure-Optical Property Relationships. *J. Phys. Chem. C* **2020**, *124*, 10744−10754.
(41) Berends, A. C.; Van der Stam, W.; Hofmann, J. P.; Bladt, E.; Meeldijk, J. D.; Bals, S.; De Mello Donega, C. Interplay between Surface Chemistry, Precursor Reactivity, and Temperature Determines Outcome of ZnS Shelling Reactions on $CuInS_2$ Nanocrystals. *Chem. Mater.* **2018**, *30*, 2400−2413.
(42) Shannon, R. D. Revised Effective Ionic Radii and Systematic Studies of Interatomic Distances. *Acta Crystallogr., Sect. A: Cryst. Phys., Diffr., Theor. Gen. Crystallogr.* **1976**, *32*, 751−767.
(43) Yuan, G.; Gomez, D. E.; Kirkwood, N.; Boldt, K.; Mulvaney, P. Two Mechanisms Determine Quantum Dot Blinking. *ACS Nano* **2018**, *12*, 3397−3405.
(44) Debnath, T.; Maiti, S.; Maity, P.; Ghosh, H. N. Subpicosecond Exciton Dynamics and Biexcitonic Feature in Colloidal $CuInS_2$ Nanocrystals: Role of In-Cu Antisite Defects. *J. Phys. Chem. Lett.* **2015**, *6*, 3458−3465.
(45) Hansen, E. C.; Bertram, S. N.; Yoo, J. J.; Bawendi, M. G. Zinc Thiolate Enables Bright Cu-Deficient Cu-In-S/ZnS Quantum Dots. *Small* **2019**, *15*, 1901462.
(46) Hughes, K. E.; Ostheller, S. R.; Nelson, H. D.; Gamelin, D. R. Copper's Role in the Photoluminescence of $Ag_{1-x}Cu_xInS_2$ Nanocrystals, from Copper-Doped $AgInS_2$ ($x \sim 0$) to $CuInS_2$ ($x = 1$). *Nano Lett.* **2019**, *19*, 1318−1325.
(47) Xia, C.; Wu, W.; Yu, T.; Xie, X.; Van Oversteeg, C.; Gerritsen, H. C.; De Mello Donega, C. Size-Dependent Band-Gap and Molar Absorption Coefficients of Colloidal $CuInS_2$ Quantum Dots. *ACS Nano* **2018**, *12*, 8350−8361.
(48) Knowles, K. E.; Hartstein, K. H.; Kilburn, T. B.; Marchioro, A.; Nelson, H. D.; Whitham, P. J.; Gamelin, D. R. Luminescent Colloidal

https://dx.doi.org/10.1021/acs.nanolett.0c04239
Nano Lett. 2021, 21, 658−665

Semiconductor Nanocrystals Containing Copper: Synthesis, Photophysics, and Applications. *Chem. Rev.* **2016**, *116*, 10820−10851.
(49) Ihara, T.; Kanemitsu, Y. Spectral Diffusion of Neutral and Charged Exciton Transitions in Single CdSe/ZnS Nanocrystals Due to Quantum-Confined Stark Effect. *Phys. Rev. B: Condens. Matter Mater. Phys.* **2014**, *90*, 195302.
(50) Hinterding, S. O. M.; Vonk, S. J. W.; Van Harten, E. J.; Rabouw, F. T. Dynamics of Intermittent Delayed Emission in Single CdSe/CdS Quantum Dots. *J. Phys. Chem. Lett.* **2020**, *11*, 4755−4761.
(51) Nelson, H. D.; Li, X.; Gamelin, D. R. Computational Studies of the Electronic Structures of Copper-Doped CdSe Nanocrystals: Oxidation States, Jahn-Teller Distortions, Vibronic Bandshapes, and Singlet-Triplet Splittings. *J. Phys. Chem. C* **2016**, *120*, 5714−5723.
(52) Müller, J.; Lupton, J. M.; Rogach, A. L.; Feldmann, J.; Talapin, D. V.; Weller, H. Monitoring Surface Charge Migration in the Spectral Dynamics of Single CdSe CdS Nanodot/Nanorod Heterostructures. *Phys. Rev. B: Condens. Matter Mater. Phys.* **2005**, *72*, 205339.
(53) Empedocles, S. A. Quantum-Confined Stark Effect in Single CdSe Nanocrystallite Quantum Dots. *Science* **1997**, *278*, 2114−2117.
(54) Park, K.; Deutsch, Z.; Li, J. J.; Oron, D.; Weiss, S. Single Molecule Quantum-Confined Stark Effect Measurements of Semiconductor Nanoparticlees at Room Temperature. *ACS Nano* **2012**, *6*, 10013−10023.
(55) Janke, E. M.; Williams, N. E.; She, C.; Zherebetskyy, D.; Hudson, M. H.; Wang, L.; Gosztola, D. J.; Schaller, R. D.; Lee, B.; Sun, C.; Engel, G. S.; Talapin, D. V. Origin of Broad Emission Spectra in InP Quantum Dots: Contributions from Structural and Electronic Disorder. *J. Am. Chem. Soc.* **2018**, *140*, 15791−15803.
(56) Hinterding, S. O. M.; Rabouw, F. T. PHoton Arrival-time STudio (PHAST). *Zenodo* 2020, DOI: 10.5281/zenodo.4354144.

https://dx.doi.org/10.1021/acs.nanolett.0c04239
Nano Lett. 2021, 21, 658−665